

Predicting Pulmonary Distension in a Virtual Patient Model for Mechanical Ventilation

Qianhui Sun*, J. Geoffrey Chase*, Cong Zhou**, Merryn H. Tawhai***, Jennifer L. Knopp*, Knut Möller****, Geoffrey M. Shaw*****

* Department of Mechanical Engineering; Dept of Mechanical Eng, Centre for Bio-Engineering, University of Canterbury, Christchurch, New Zealand (e-mail: qianhui.sun@pg.canterbury.ac.nz; geoff.chase@canterbury.ac.nz; cong.zhou@nwpu.edu.cn; jennifer.knopp@canterbury.ac.nz)

** School of Civil Aviation, Northwestern Polytechnical University, China

*** Auckland Bioengineering Institute, The University of Auckland, Auckland, New Zealand (e-mail: m.tawhai@auckland.ac.nz)

**** Institute for Technical Medicine, Furtwangen University, Villingen-Schwenningen, Germany (e-mail: Knut.Moeller@hs-furtwangen.de)

***** Department of Intensive Care, Christchurch Hospital, Christchurch, New Zealand (e-mail: geoff.shaw@cdhb.health.nz)

Abstract: Recruitment maneuvers (RMs) following with positive-end-expiratory-pressure (PEEP) have proved effective in recruiting lung volume and preventing alveoli collapse. To date, standards for optimal patient-specific PEEP are unknown, resulting in variability in care and reduced outcomes, both indicating the need for personalized care. This research extends a well-validated virtual patient model by adding novel elements to model, which is able to utilize bedside available respiratory data, without increasing modelling complexity, to predict patient-specific lung distension and thus to minimise barotrauma risk. Prediction accuracy and robustness are validated against clinical data from 18 volume controlled ventilation (VCV) patients at 7 different baseline PEEP levels (0 to 12cmH₂O), where predictions were made up to 12cmH₂O of PEEP ahead. Using an exponential basis function set for prediction yields an absolute median peak inspiratory pressure prediction error of 1.50cmH₂O for 623 prediction cases. Comparing predicted and clinically measured distension prediction in VCV demonstrated consistent, robust high accuracy with R²=0.90 (623 predictions), which is a measurable improvement in prediction error compared to predictions without using the proposed distension function (R²=0.82). Moreover, the R² value increases to 0.93-0.95 if only clinically relevant ΔPEEP steps (2-6cmH₂O) are considered with an overall median absolute error in peak pressure prediction of 1.04cmH₂O. Overall, the results demonstrate the potential and significance for accurately capturing distension mechanics, allowing better risk assessment, as well as extending and more fully validating this virtual mechanical ventilation patient model.

Keywords: Virtual Patient; Digital Twin; Mechanical ventilation; Critical Care; Basis function; Prediction; Elastance; Lung distension; VILI; Pressure-Volume loop.

1. INTRODUCTION

Volume-controlled ventilation (VCV) controls flow to deliver a targeted tidal volume (Ashworth et al., 2018). However, there is risk of ventilator induced lung injury (VILI) if the resulting uncontrolled airway pressure is too high (Cadi et al., 2008). This risk increases during recruitment maneuvers (RMs) changing positive-end-expiratory-pressure (PEEP) to recruit lung volume, which are common in managing acute respiratory distress syndrome (ARDS) and respiratory failure patients (Fodor et al., 2019). However, sub-optimal PEEP, resulting in excessive or insufficient pressure, can lead to VILI, increasing morbidity and mortality (Carney et al., 2005).

To date, there is no set method to determine the optimal patient-specific PEEP, creating variability in care and risk (Chase et al., 2018; Chiew et al., 2011). Model-based

approaches are one means to personalize care (Chase et al., 2018), and assess lung mechanics (Sundaresan & Chase, 2012). However, while there are many models, very few accurately predict pulmonary mechanics at a new PEEP level (Morton et al., 2019a; Morton et al., 2019b; Morton et al., 2020; Zhou et al., 2021). An accurate, predictive lung mechanics model would let clinicians test new mechanical ventilation (MV) settings without risk.

Basis functions have been proposed for targeted biomedical simulation and prediction (Langdon et al., 2018; Morton et al., 2018; Morton et al., 2019b; Morton et al., 2020; Zhou et al., 2021). Well-defined, they offer additional, model-based insight into physiological mechanics (Langdon et al., 2018; Morton et al., 2019b; Morton et al., 2020). A nonlinear, physiologically-relevant hysteresis loop model (HLM) using an exponential basis function set accurately captured and

predicted the evolution of lung mechanics as MV settings change for both VCV and pressure controlled ventilation (Zhou et al., 2021), but did not capture distension in VCV, which is important in directly managing the risk of VILI.

This research proposes an additional novel basis function to extend the model in (Zhou et al., 2021), aiming to capture patient-specific over-distension. Overall outcome is improved with a lower median peak inspiratory pressure (PIP) prediction error and much narrower error range compared with predictions without proposed distension function, which thus provides significant new utility for clinical care.

2. METHODS

2.1 HLM lung mechanics model

The dynamic equation of motion for the HLM lung mechanics model is defined (Zhou et al., 2021):

$$\dot{V} + R\dot{V} + K_e V + K_{h1} V_{h1} + K_{h2} V_{h2} = f_v(t) + PEEP \quad (1)$$

where V is the volume of air delivered to the lungs, V_{h1} and V_{h2} are hysteretic volume response during inspiration and expiration, respectively, K_e represents the alveolar recruitment elastance, named $k2$ in this approach, K_{h1} and K_{h2} , are determined by two nonlinear hysteretic springs for alveolar hysteresis elastance during inspiration and expiration, respectively, R is the airway resistance, $PEEP$ is the positive end-expiratory pressure, and $f_v(t)$ is the steady-state input force. Detailed formulations for calculating each parameter can be found in (Zhou et al., 2021).

2.2 P-V loop identification

At the first baseline $PEEP_1$ level, the hysteresis loop analysis method (HLA) is used to identify elastance values for further prediction. For expiration, 2 segments are identified with two elastances, $k3$ and $k4$, used for dynamic functional residual volume prediction (Zhou et al., 2021) and not discussed in this study. For inspiration, the half cycle is first divided into 2 segments, with $k1$ and $k2$. Subsequently, the $k2$ segment is assessed to find a potential, increased stiffness (reduced compliance) third segment, $k2end$, which will use the newly proposed basis function prediction procedure to capture over-distension as $PEEP$ rises. An identification example is shown in Figure 1 with a clinical PV loop.

2.3 Basis functions for elastance prediction

After HLA identification, an exponential basis function set used in prior studies (Laufer et al., 2017; Morton et al., 2018; Zhou et al., 2021), is used to predict the evolution of recruitment elastance at higher $PEEP_i$ ($k2_i$, $i > 1$). It assumes elastance has a bowl shape across $PEEP$ (Zhou et al., 2021):

$$k2_i = \left(\frac{PEEP_i}{k1} + \frac{k2_1}{k1} * e^{b * \frac{PEEP_i}{k1}} \right) * k1 \quad (2)$$

$$b = \frac{k1}{PEEP_1} * \log \frac{k2_1 - PEEP_1}{k2_1} \quad (3)$$

Where b is the exponential rate of recruitment, $k1$ and $k2_1$ are the identified values via HLA from baseline $PEEP_1$, and $PEEP_i$ ($i > 1$) is the predicted $PEEP$ level. Figure 2 shows the

the way for identified $k2_1$ and baseline $PEEP$ level affect the yielding $k2_i$ prediction across $\Delta PEEP$ intervals.

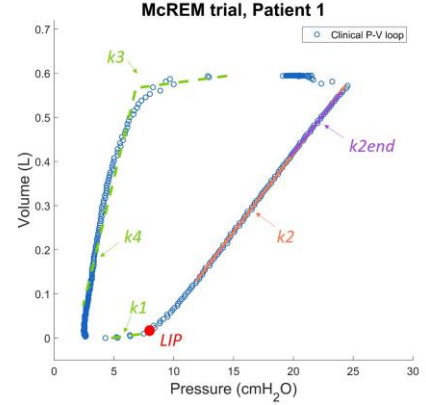
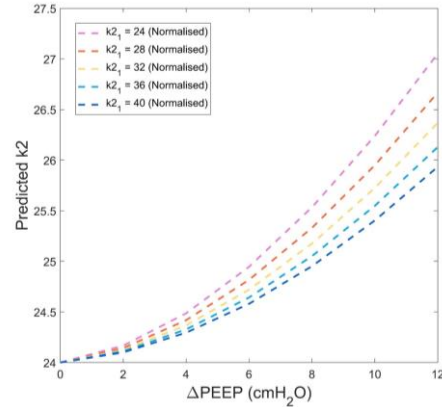
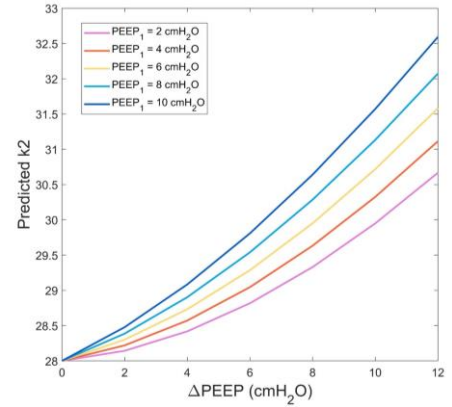


Figure 1 Example of HLA identification for a measured clinical P-V loop at a baseline $PEEP = 2\text{cmH}_2\text{O}$ for Patient 1, while the lower inflection point (LIP) is shown.



(a) Identified $k2_1$ by initial value normalised



(b) Baseline $PEEP_1$ level ($PEEP_1$)

Figure 2 The influence of (a) identified $k2_1$ (initial value normalised) and (b) baseline $PEEP_1$ terms in resulting $k2_i$ prediction.

At the same time, the evolution of distension at higher $PEEP$ levels ($k2end_i$, $i > 1$) is also predicted. In this approach, end expiratory volume ($EELV_1$) and expiratory tidal volume ($PIV_1 - EELV_1$, with PIV_1 peak inspiratory volume) identified at baseline $PEEP$ are assumed to interact with predicted $k2_i$ to predict $k2end$ distension elastance. A new basis function is thus proposed to capture and predict the evolution of over-distension during HLM modelling:

$$k2end_i = \left(\frac{PEEP_i}{k2_i} + \frac{k2end_1}{k2_1} * (\theta1 + \theta2^2) \right) * k2_i \quad (4)$$

$$\theta1 = \frac{k2end_1 - PEEP_1}{k2end_1} \quad (5)$$

$$\theta2 = \Delta PEEP * \frac{EELV_1}{PIV_1 - EELV_1} \quad (6)$$

Where $\Delta PEEP = PEEP_i - PEEP_1$. Figure 3 shows a sketch of basis function terms over PEEP for $k2end$ evolution.

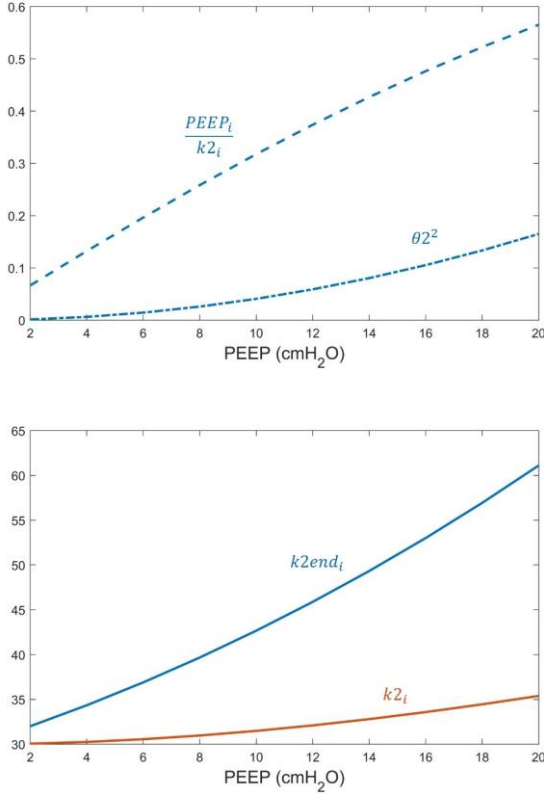


Figure 3 Upper panel illustrates the contribution of each term and how they change over PEEP for $k2end$ prediction in (4)-(6), while lower panel presents the yielding $k2end_i$ with predicted $k2_i$.

2.4 Patient data

Ventilation data from 18 ventilated ICU patients from the McREM trial (Stahl et al., 2006) is used to validate the basis function proposed. All 18 patients were fully sedated and intubated under invasive VCV, with tidal volume set to 8 ± 2 ml/kg based on ideal body weight (Stahl et al., 2006). The McREM trial was conducted across eight German university ICUs from September 2000 to February 2002. All 18 patients were ventilated with a Draeger Evita 4 ventilator. During ventilation, an end-inspiratory hold of 0.2s is applied for each breath and data were sampled at 125 Hz.

One incremental staircase RM with $\Delta PEEP = 2\text{cmH}_2\text{O}/\text{step}$ was performed for each patient starting at $0\text{cmH}_2\text{O}$. The prediction procedure is applied for higher PEEP levels ($i = 2, \dots, 7$) after identification at baseline PEEP ($i = 1$). To test the robustness and generality of the HLM model and basis function sets, prediction tests are applied across a range of

baseline PEEP = 0, 2, 4, 6, 8, 10, and $12\text{cmH}_2\text{O}$ with a further 6 prediction steps ($2\text{cmH}_2\text{O}$ interval) from each baseline level, yielding a maximum value for $\Delta PEEP = 2 \times 6$ steps = $12\text{cmH}_2\text{O}$. There are thus a total of 623 predictions across the 7 baseline PEEP test groups and patients. Demographics for the patients can be found in (Zhou et al., 2021).

3. RESULTS

The cumulative distribution function (CDF) plots in Figure 4 (623 predictions) show improved prediction accuracy using the proposed $k2end$ function. Overall, 90% of PIP prediction errors are within $3.95\text{cmH}_2\text{O}$, compared with $4.76\text{cmH}_2\text{O}$ (90% errors) without $k2end$. Without $k2end$, R^2 decreases from 0.90 to 0.82 and overshooting bias decreases from 60% to 25%, where underestimated PIP prediction could lead to selecting a higher PEEP, increasing the risk of VILI.

Boxplots for absolute PIP prediction errors with and without $k2end$ are presented in Figure 5. Including $k2end$ results in a lower overall median error, $1.50\text{cmH}_2\text{O}$ compared with $1.80\text{cmH}_2\text{O}$, and a much narrower error range for all 7 baseline PEEP groups, both indicating the added basis function for over-distention enables a better representation of lung mechanics as PEEP rises. Where baseline PEEP = $0-2\text{cmH}_2\text{O}$, median errors are lower without $k2end$. However, maximum error is still much larger, $15.39\text{cmH}_2\text{O}$, compared to $5.71\text{cmH}_2\text{O}$ with proposed $k2end$ function.

Figures 4-5 show the novel added $k2end$ prediction presented captures possible over-distention and barotrauma in VCV patients. Assessing only clinically relevant $\Delta PEEP = 2-6\text{cmH}_2\text{O}$ (1-3 prediction steps). Table 1 shows higher R^2 values of $R^2 = 0.93-0.95$ compared to $R^2 = 0.88-0.93$ without $k2end$ while the median and 90% of the PIP prediction errors are also provided. The statistics by column in Table 1 are cumulative for 1 step forward, 1 step and 2 steps forward together, up to all 6 steps forward for the whole cohort, yielding 122, 241, 356, 460, 550, and 623 prediction case respectively (6 steps column presents the total cohort values).

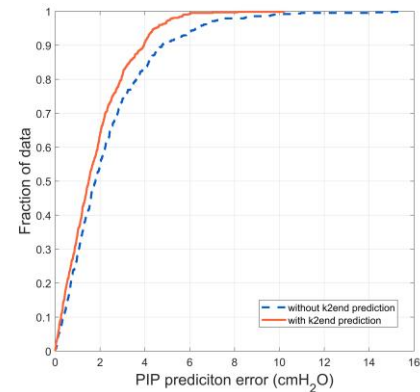
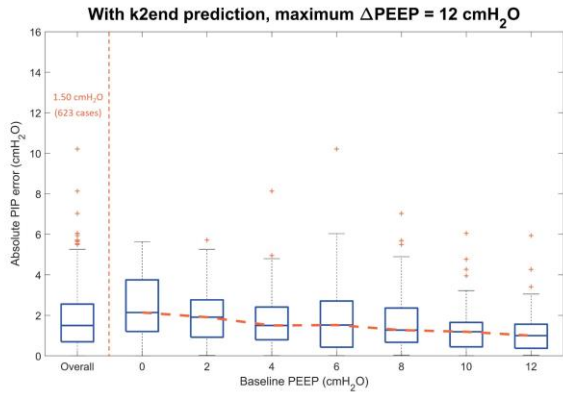
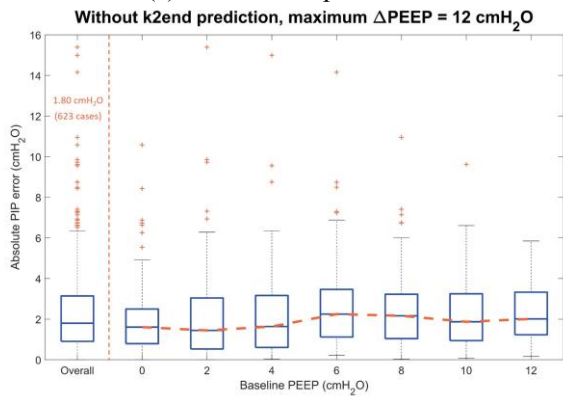


Figure 4 The CDF plot for absolute PIP prediction errors with (solid line) and without (dash line) proposed $k2end$ prediction for 623 cases.



(a) With $k2end$ prediction



(b) Without $k2end$ prediction

Figure 5 Boxplots for PIP prediction errors over 7 baseline PEEPs for (a) with $k2end$ prediction and (b) without $k2end$ prediction.

A prediction example is shown in Figure 7 for Patient 6 at baseline PEEP = 6cmH₂O with Δ PEEP = 12cmH₂O, so it is predicting response at PEEP = 18cmH₂O, the maximum prediction interval and at a PEEP level where distension can appear and be significant for some patients. It shows far better accuracy using $k2end$ and the noticeable distention is captured well, despite the large prediction interval, and lack of distension at the original PEEP = 6cmH₂O data. More importantly, the proposed basis function for $k2end$ prediction provides a patient specific replication of distention impact, as the amount of distention can be significantly varied from patient to patient even with similar ratio of change in $k2$, for example shown in Figure 6.

Table 1 - R² value, PIP prediction error (cmH₂O) in median and within 90% range across different cumulative collections of further prediction steps intervals (2cmH₂O for each step).

	1 step	2 steps	3 steps	4 steps	5 steps	6 steps
With $k2end$ prediction						
R ²	0.95	0.95	0.93	0.92	0.91	0.9
median	0.86	0.98	1.19	1.32	1.41	1.50
90% within	2.27	2.76	2.93	3.14	3.55	3.95
Without $k2end$ prediction						
R ²	0.93	0.91	0.88	0.86	0.84	0.82
median	1.27	1.36	1.47	1.58	1.67	1.80
90% within	2.86	3.42	3.84	4.28	4.57	4.76

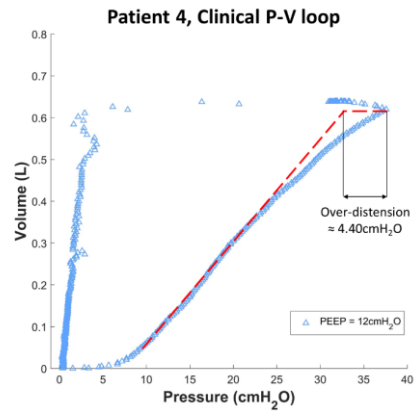
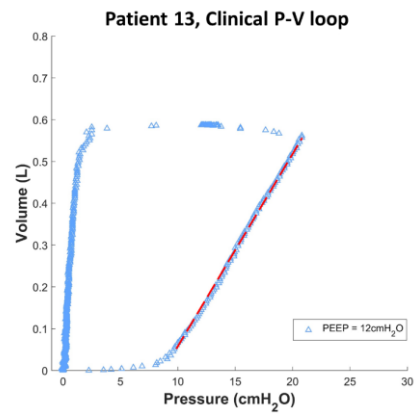


Figure 6 Examples for Patient 4 (lower panel) and Patient 13 (upper panel) at PEEP = 12cmH₂O, with a similar changing ratio (~1.49) from baseline PEEP = 0cmH₂O, while over-distension can be varied from nearly 0 to 4.40cmH₂O.

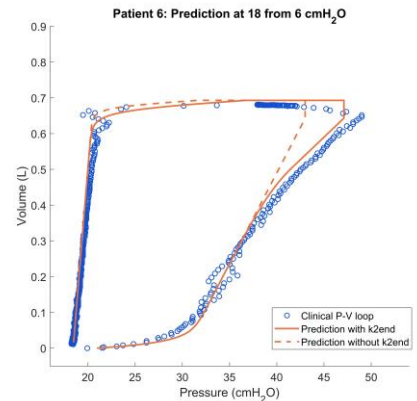


Figure 7 Example for difference without (dash line) and with proposed $k2end$ prediction (solid line) for Patient 6 at baseline PEEP = 6cmH₂O and Δ PEEP = 12cmH₂O, so prediction made for PEEP = 18cmH₂O where distension can be more significant.

4. DISCUSSION

As in prior works (Jonson et al., 1999; Sundaresan & Chase, 2012; Zhou et al., 2021), the segment of the P-V loop between the LIP and upper inflection point (UIP) is treated as linear, while the segment above UIP until the end of inspiration ($k2end$) is specially identified as a separate linear segment in this approach, which is treated as curvilinear and constant over PEEP in (Jonson et al., 1999) and not considered in other works (Sun et al., 2020; Sundaresan & Chase, 2012). Using the UIP as an upper limit before distension has been

approximated in clinical studies (Maggiore et al., 2003; Stenqvist & Odenstedt, 2007), but this study is the first model-based effort to quantify and to predict distension. After identification, evolution of k_2 and k_{2end} , are predicted using (2)-(6), where prediction accuracy is the key to clinical utility in guiding MV care (Chase et al., 2018; Morton et al., 2019a). Identifying and predicting k_{2end} is a novel model capability and a key feature of this approach as it directly captures potential barotrauma in VCV and over-distension and thus the risk of VILI.

The amount of over-distension is a critical factor in VCV care, as recruiting more lung when over-distension occurs also means healthy lung units may be damaged (Gomez-Laberge et al., 2012; Vieira et al., 1998). As shown in Figure 6, the amount of distension can be distinct from patient to patient, even under similar k_2 changing ratio and Δ PEEP. Thus, distension and k_{2end} can be even more patient-specific than k_2 , but provide significant new lung mechanics insight to optimise VCV while also helping reduce the risk of VILI.

Some lung imaging methods, such as computed tomography scans, are able to identify distension in patient lungs after clinical treatment (Cereda et al., 2013; Fumagalli et al., 2019). However, regardless of the availability and the requirement of additional devices, none of these imaging methods enable prediction of over-distension based on images at a single PEEP level, reinforcing the potential clinical utility of a model-based digital twin or virtual patient approach (Chase et al., 2018) as presented here.

Overall PIP prediction errors with proposed k_{2end} function are improved with a narrow range, as shown in Figures 4-5, with decreased median error from 1.80cmH₂O to 1.50cmH₂O and fewer, smaller outliers, which lowers potential critical risks for patients and thus increase clinical application confidence. As baseline PEEP increases, the median error for PIP prediction with proposed k_{2end} function, as presented in Figure 5 (a), tends to decrease while baseline PEEP increases. This outcome is possibly a result of slightly fewer prediction cases as baseline PEEP increases due to clinical treatment, as well as a more likely occurrence of distention at higher baseline PEEP. As comparison, the median prediction errors without proposed k_{2end} function, as shown in Figure 5 (b), are relatively higher in larger baseline PEEP levels. Given the large number of predictions (623 cases), the lower error at clinically relevant PEEP levels is more important. Equally, the higher prediction errors at lower baseline PEEP, from 0 to 4cmH₂O, are relatively less critical and harmful for patients compared with higher baseline PEEP where higher PIP and higher PIP prediction errors increases harming risk. Moreover, the prediction performance across different Δ PEEP intervals, as shown in Figure 5, is presented with improvement.

A few large outliers still occurred as shown in Figure 5 (a). However, these all occurred in Patient 16 for large Δ PEEP = 6-12cmH₂O. Patient 16 is the only patient in the McREM trial with an extremely low P/F ratio = 75, while all others are all above 140. A P/F ratio lower than 100 can be the indicator of very severe ARDS and is a predictor of mortality (Adams et al., 2020). Thus, this patient has much worse pulmonary

condition compared to the other 17 McREM patients, many of whom also meet broad less severe ARDS definitions (The ARDS Definition Task Force, 2012). Excluding this patient (27 prediction cases in 7 baseline PEEP groups), all PIP prediction errors are within 5.95cmH₂O from the remaining 596 prediction cases, with 1.48cmH₂O median error. More importantly, if only the first, clinically relevant 1-3 PEEP steps are considered, it yields $R^2=0.93-0.95$ (compared to $R^2=0.88-0.93$) and median error in 0.86-1.19cmH₂O (compared with 1.27-1.47cmH₂O).

The newly presented k_{2end} parameter and its prediction accurately only captures over-distension for 4 of 7 baseline PEEP prediction groups. However, as presented in Figure 4, the overall prediction across all 7 groups is still improved with the proposed k_{2end} parameter, even for a patient with much worse lung condition (P/F<100), which shows the importance of including a separate k_{2end} prediction to capture over distension, and offers a promising, clinically useful prediction method, particularly at higher PEEP levels where peak pressures will be high enough for distension to be likely. More importantly, prediction performance accessed across 18 ventilated patients at a wide range of different baseline PEEP levels (from 0 to 12cmH₂O) with Δ PEEP prediction intervals up to 12cmH₂O. While being effective and reducing modelling effort, the overall outcome shows the physiological relevant basis function sets offer the possibility for accurate and simpler lung mechanics prediction, especially over clinically realistic Δ PEEP=2-6cmH₂O intervals.

5. CONCLUSIONS

In conclusion, this study presents an extended and more accurate virtual patient model for volume controlled ventilation, including novel terms to capture and predict the clinically important risk of over-distension and thus the risk of VILI. It presents the promising ability of physiologically relevant basis functions for lung mechanics prediction at a single baseline PEEP breath, which is computationally simple and non-invasive as it requires no new or other measurements. Increased data and prospective clinical validation are still required to translate this MV virtual patient modelling methodology from research into clinical implementation to personalise and optimise MV care.

6. ACKNOWLEDGEMENTS

This work was supported by the NZ Tertiary Education Commission (TEC) fund MedTech CoRE (Centre of Research Excellence; #3705718) and the NZ National Science Challenge 7, Science for Technology and Innovation (2019-S3-CRS). The authors also acknowledge support from the EU H2020 R&I programme (MSCA-RISE-2019 call) under grant agreement #872488 — DCPM.

REFERENCES

Adams, JY, Rogers, AJ, Schuler, A, Marelich, GP, Fresco, JM, Taylor, SL, Riedl, AW, Baker, JM, Escobar, GJ & Liu, VX 2020, 'Association Between Peripheral Blood Oxygen Saturation (SpO₂)/Fraction of Inspired Oxygen (FiO₂) Ratio Time at Risk and Hospital

- Mortality in Mechanically Ventilated Patients', *The Permanente journal*, vol. 24, p. 19.113.
- Ashworth, L, Norisue, Y, Koster, M, Anderson, J, Takada, J & Ebisu, H 2018, 'Clinical management of pressure control ventilation: An algorithmic method of patient ventilatory management to address "forgotten but important variables"', *Journal of Critical Care*, vol. 43, pp. 169-182.
- Cadi, P, Guenoun, T, Journois, D, Chevallier, J-M, Diehl, J-L & Safran, D 2008, 'Pressure-controlled ventilation improves oxygenation during laparoscopic obesity surgery compared with volume-controlled ventilation', *BJA: British Journal of Anaesthesia*, vol. 100, no. 5, pp. 709-716.
- Carney, D, DiRocco, J & Nieman, G 2005, 'Dynamic alveolar mechanics and ventilator-induced lung injury', *Crit Care Med*, vol. 33, no. 3, pp. S122-S128.
- Cereda, M, Emami, K, Xin, Y, Kadlecsek, S, Kuzma, NN, Mongkolwisetwara, P, Profka, H, Pickup, S, Ishii, M, Kavanagh, BP, Deutschman, CS & Rizi, RR 2013, 'Imaging the interaction of atelectasis and overdistension in surfactant-depleted lungs', *Critical care medicine*, vol. 41, no. 2, pp. 527-535.
- Chase, JG, Preiser, J-C, Dickson, JL, Pironet, A, Chiew, YS, Pretty, CG, Shaw, GM, Benyo, B, Moeller, K, Safaei, S, Tawhai, M, Hunter, P & Desaive, T 2018, 'Next-generation, personalised, model-based critical care medicine: a state-of-the art review of in silico virtual patient models, methods, and cohorts, and how to validation them', *BioMedical Engineering OnLine*, vol. 17, no. 1, p. 24.
- Chiew, YS, Chase, JG, Shaw, GM, Sundaresan, A & Desaive, T 2011, 'Model-based PEEP optimisation in mechanical ventilation', *BioMedical Engineering OnLine*, vol. 10, no. 1, p. 111.
- Fodor, GH, Bayat, S, Albu, G, Lin, N, Baudat, A, Danis, J, Peták, F & Habre, W 2019, 'Variable Ventilation Is Equally Effective as Conventional Pressure Control Ventilation for Optimizing Lung Function in a Rabbit Model of ARDS', *Frontiers in Physiology*, vol. 10, no. 803
- Fumagalli, J, Santiago, RRS, Teggia Droghi, M, Zhang, C, Fintelmann, FJ, Troschel, FM, Morais, CCA, Amato, MBP, Kacmarek, RM, Berra, L & Investigators, obotLRT 2019, 'Lung Recruitment in Obese Patients with Acute Respiratory Distress Syndrome', *Anesthesiology*, vol. 130, no. 5, pp. 791-803.
- Gomez-Laberge, C, Arnold, JH & Wolf, GK 2012, 'A Unified Approach for EIT Imaging of Regional Overdistension and Atelectasis in Acute Lung Injury', *IEEE Transactions on Medical Imaging*, vol. 31, no. 3, pp. 834-842.
- Jonson, B, Richard, J-C, Straus, C, Mancebo, J, Lemaire, F & Brochard, L 1999, 'Pressure-Volume Curves and Compliance in Acute Lung Injury', *American Journal of Respiratory and Critical Care Medicine*, vol. 159, no. 4, pp. 1172-1178.
- Langdon, R, Docherty, PD, Mansell, EJ & Chase, JG 2018, 'Accurate and precise prediction of insulin sensitivity variance in critically ill patients', *Biomedical Signal Processing and Control*, vol. 39, pp. 327-335.
- Laufer, B, Docherty, PD, Knörzer, A, Chiew, YS, Langdon, R, Möller, K & Chase, JG 2017, 'Performance of variations of the dynamic elastance model in lung mechanics', *Control Engineering Practice*, vol. 58, pp. 262-267.
- Maggiore, SM, Richard, JC & Brochard, L 2003, 'What has been learnt from P/V curves in patients with acute lung injury/acute respiratory distress syndrome', *Eur Respir J*, vol. 22, no. 42, suppl, pp. 22s-26.
- Morton, SE, Dickson, J, Chase, JG, Docherty, P, Desaive, T, Howe, SL, Shaw, GM & Tawhai, M 2018, 'A virtual patient model for mechanical ventilation', *Comput Methods Programs Biomed*, vol. 165, pp. 77-87.
- Morton, SE, Knopp, JL, Chase, JG, Docherty, P, Howe, SL, Möller, K, Shaw, GM & Tawhai, M 2019a, 'Optimising mechanical ventilation through model-based methods and automation', *Annual Reviews in Control*, vol. 48, pp. 369-382.
- Morton, SE, Knopp, JL, Chase, JG, Möller, K, Docherty, P, Shaw, GM & Tawhai, M 2019b, 'Predictive Virtual Patient Modelling of Mechanical Ventilation: Impact of Recruitment Function', *Annals of Biomedical Engineering*, vol. 47, no. 7, pp. 1626-1641.
- Morton, SE, Knopp, JL, Tawhai, MH, Docherty, P, Heines, SJ, Bergmans, DC, Möller, K & Chase, JG 2020, 'Prediction of lung mechanics throughout recruitment maneuvers in pressure-controlled ventilation', *Computer Methods and Programs in Biomedicine*, vol. 197, p. 105696.
- Stahl, CA, Möller, K, Schumann, S, Kuhlen, R, Sydow, M, Putensen, C & Guttmann, J 2006, 'Dynamic versus static respiratory mechanics in acute lung injury and acute respiratory distress syndrome', *Crit Care Med*, vol. 34, no. 8, pp. 2090-2098.
- Stenqvist, O & Odenstedt, H 2007, 'Alveolar Pressure/volume Curves Reflect Regional Lung Mechanics', *Intensive Care Medicine*, pp. 407-414.
- Sun, Q, Zhou, C & Chase, JG 2020, 'Parameter updating of a patient-specific lung mechanics model for optimising mechanical ventilation', *Biomedical Signal Processing and Control*, vol. 60, p. 102003.
- Sundaresan, A & Chase, JG 2012, 'Positive end expiratory pressure in patients with acute respiratory distress syndrome – The past, present and future', *Biomedical Signal Processing and Control*, vol. 7, no. 2, pp. 93-103.
- The ARDS Definition Task Force 2012, 'Acute respiratory distress syndrome: The berlin definition', *JAMA: The Journal of the American Medical Association*, vol. 307, no. 23, pp. 2526-2533.
- Vieira, SRR, Puybasset, L, Richecoeur, J, Lu, QIN, Cluzel, P, Gusman, PB, Coriat, P & Rouby, J-J 1998, 'A Lung Computed Tomographic Assessment of Positive End-Expiratory Pressure-induced Lung Overdistension', *American Journal of Respiratory and Critical Care Medicine*, vol. 158, no. 5, pp. 1571-1577.
- Zhou, C, Chase, JG, Knopp, J, Sun, Q, Tawhai, M, Möller, K, Heines, SJ, Bergmans, DC, Shaw, GM & Desaive, T 2021, 'Virtual patients for mechanical ventilation in the intensive care unit', *Computer Methods and Programs in Biomedicine*, vol. 199, p. 105912.